

Effect of Plasticizer on the Crystallization Behavior of Poly(lactic acid)

Hanwen Xiao,¹ Wei Lu,¹ Jen-Taut Yeh^{1,2,3}

¹Ministry of Education Key, Laboratory of the Green Preparation and Application of Functional Materials, Institute of Composite Materials, Faculty of Materials Science and Engineering, Hubei University, Wuhan 430062, China

²Key Laboratory of Green Processing and Functional Textiles of New Textile Materials (Wuhan University of Science and Engineering), Ministry of Education, Wuhan, China

³Department and Graduate School of Polymer Engineering, National Taiwan University of Science and Technology, Taipei, Taiwan

Received 29 June 2008; accepted 26 December 2008

DOI 10.1002/app.29955

Published online 13 March 2009 in Wiley InterScience (www.interscience.wiley.com).

ABSTRACT: In this article, the spherulitic morphology and growth rate of the neat and plasticized poly(lactic acid) (PLA) with triphenyl phosphate (TPP) were compared and analyzed by polarizing optical microscopy with hot stage at a temperature range of 100–142°C. The spherulitic morphology of the neat PLA underwent a series of changes such as the typical Maltese Cross at less than 132°C, the disappearance of the Maltese Cross at 133°C, the irregular and distorted spherulites at higher than 134 and 142°C, respectively. For plasticized PLA, the spherulitic morphology exhibited the same changes as neat PLA, but these changes were shifted to lower temperature when compared with neat PLA. In the case of the spherulitic growth, neat PLA had the maximum value of 0.28 $\mu\text{m/s}$ at 132°C, and plasticized PLA had higher values than that of neat PLA. Further analysis based on the Lauritzen–

Hoffman theory was presented and results showed that the values of nucleation parameter K_g increased with TPP content. The crystallization behavior of PLA was analyzed by differential scanning calorimetry and wide-angle X-ray diffraction. The results showed that the degree of crystallinity of plasticized PLA markedly increased when compared with neat PLA sharply with the incorporation of plasticizer. The crystallization kinetics for the neat and plasticized PLA under isothermal crystallization at 114°C was described by the Avrami equation and the Avrami exponent is close to 2, implying that the crystallization mechanism did not change. © 2009 Wiley Periodicals, Inc. *J Appl Polym Sci* 113: 112–121, 2009

Key words: biodegradable polymer; crystallization kinetics; equilibrium melting point; morphology

INTRODUCTION

Research in biodegradable polymers has received increased attention in recent years because of their wide applications in environmental protection and the maintenance. Among them, aliphatic polyester is one of the most popular and important biodegradable polymers because they are readily susceptible to biological attack.¹

Poly(lactic acid) (PLA), a biodegradable aliphatic polyester, produced from renewable resources has received much attention in the research of biodegradable polymers.^{2,3} PLA has good mechanical properties such as high mechanical strength, thermo-plasticity, and fabricability.⁴ However, PLA has some shortcomings, such as hard and brittle mechanical properties and a relatively low crystallization rate, which restrict its development and

practical application. Therefore, considerable efforts have been made to improve the properties of PLA so as to compete with low-cost and flexible commodity polymers. One of these attempts was carried out by means of plasticization. Varying types of plasticizers such as poly(ethylene glycol) (PEG),^{5–11} poly(propylene glycol) (PPG),^{12,13} oligomeric lactic acid (OLA),⁶ glycerol,⁶ citrate ester,^{14,15} triacetone,¹⁵ tributyl citrate,¹⁶ acetyltriethyl citrate, tributyl citrate oligomers, diethyl bishydroxymethyl malonate-oligomers,¹⁷ glucosemonoesters, and partial fatty acid ester^{18,5} were used to improve the flexibility and impact resistance of PLA. PEG is the most studied plasticizer for PLA, and the efficiency of plasticization was increased with decreasing molecular weight. The T_g was shown to be depressed from 58°C for pure PLA to 41 and 30°C, respectively, at 10 and 20% PEG loading levels for PEG molecular weight of 1500.⁶ The T_g can be further depressed using a lower PEG molecular weight of 400, to 30 and 12°C, respectively, and the elongations at break were 26 and 160%, respectively, at those same PEG loading levels. In another study, it was also shown that low-molecular-weight PEG could accelerate the spherulite growth rate.⁸ While using high PEG

Correspondence to: J.-T. Yeh (jyeh@tx.ntust.edu.tw).

Contract grant sponsor: Ministry of Education Key Laboratory for the Green Preparation and Application of Functional Materials.

concentration, e.g., 30 wt %, blends of PLA and PEG could undergo phase separation, depending on PEG's molecular weight. One of the reasons of instability of PLA/PEG blends is crystallization of PEG, which depletes the amorphous phase of the plasticizer.⁷ Martin and Avérous studied the plasticization and properties of PLA plasticized with OLA and glycerol⁶ and compared OLA and glycerol with other plasticizer, such as citrate ester and PEG with different average molecular weights. Conclusions were drawn that glycerol was the least efficient plasticizer, and OLA and the lower molecular weight PEG (PEG 400) gave the best result.⁶ Kulinski et al.¹² reported plasticization of amorphous PLA with two PPGs differing in molecular weight. PPG with higher molecular weight separated from amorphous PLA when its content reached 12.5 wt %, but tiny liquid pools of PPG did not deteriorate the ability of the blend to plastic deformation.

As far as triphenyl phosphate (TPP) was concerned, it was both flame-retardant for poly(acrylonitrile-butadiene-styrene), poly(methylmethacrylate), and poly(ethylene terephthalate), and plasticizer for poly(vinyl chloride), flexibility polyurethane foam, and rubber^{19–22}; however, up to date, PLA plasticized with TPP has not been reported in the literature. In this article, the study was mainly focused on the crystallization behavior of the neat and plasticized PLA. The detail study of the plasticization effect of TPP on PLA had been carried out and will be reported in a separate paper. It is well known that the crystallinity plays an important role in the physical properties. Meanwhile, the crystalline structure and morphology of semicrystalline polymers are also influenced greatly by the thermal history. Therefore, much more attention should be directed to the crystallization kinetics study. In this work, spherulitic morphology and growth rate, crystal structure, and the crystallization kinetics of the neat and PLA plasticized with TPP were studied by differential scanning calorimetry (DSC), polarizing optical microscopy (POM), and wide-angle X-ray diffraction (WAXD) in detail. It is expected that the results will be helpful for a better understanding of the relationship between structure and property of the neat and plasticized PLA.

EXPERIMENTAL

Materials

The commercial PLA in pellet form (Natureworks PLA 4032D) exhibits a density of 1.25 g/cm³, a weight-average molecular weight of 207 kDa, polydispersity of 1.74 (gel permeation chromatography analysis), and a glass transition temperature and melting point of 60 and 168°C [differential scanning calorimeter (DSC) analysis], respectively. TPP (C.P. grade;

Kelong Chemical Reagent Factory, Chengdu, China) was used as PLA plasticizer, which had a molecular weight of 326.3 g/mol and a melting point of 48°C.

Sample preparation

The neat PLA was predried in vacuum oven at 80°C for 24 h before use. PLA and TPP were mixed together with different weight ratios of 100/0, 90/10, 80/20, and 70/30 in Haake internal mixer (Rheomix 600P, Germany) with Roller-Rotors R600 for 3 min. The mixing rollers were maintained at 90 rpm, and the temperature was set at 185°C. Then, the melts were compressed to films with a thickness of around 0.5 mm for 3 min at 185°C and 10 MPa for the neat and plasticized PLA, respectively.

Thermal analysis

The thermal characteristics of the neat and plasticized PLA were determined using a differential scanning calorimeter (DSC Q100, TA instrument, USA) in nitrogen atmosphere (circulation). Samples (ca. 10 mg) were cut from a sample and placed in sealed aluminum pans. For each sample, the following thermal cycles was applied: a first scan was made from room temperature to 185°C for 3 min to destroy any thermal history. Then the sample was cooled to -50°C rapidly. The actual measurement was performed during a second heating from -50 to 200°C at a heating rate of 10°C/min. A nitrogen flow was maintained throughout the test. The glass transition temperature (T_g), the cold crystallization temperature (T_{cc}), the degree of crystallinity (x_c), the degree of cold crystallinity (x_{cc}), and the melting temperature (T_m) were determined in the second heating scan. Based on the heat of fusion of 100% crystallinity of PLA (93 J/g),²³ the degree of crystallinity or the degree of cold crystallinity of PLA was calculated from the melting endotherms of the samples and normalized with respect to the composition of each component in the plasticized PLA.

The equilibrium melting temperature (T_m^0) of the neat and plasticized PLA are determined by extrapolation to the lines of $T_m = T_c$ according to the Hoffman-Weeks equation.²⁴ Samples were heated to 185°C and maintained for 3 min and then cooled at 50°C/min and crystallized at the temperature range of 120–142°C for PLA sample and 110–132°C for plasticized PLA samples, respectively. At each temperature, annealing lasts for 10 h in nitrogen atmosphere, and then the samples were cooled to room temperature at 40°C/min and heated to 200°C at 10°C/min for the determination of the melting points.

The isothermal crystallization from the melt was also examined by DSC. The samples were cooled to 114°C at a cooling rate of 50°C/min to crystallize the

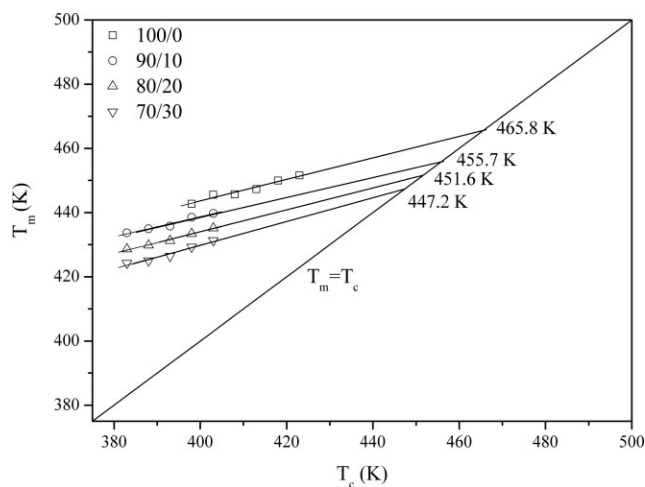


Figure 1 Hoffman–Weeks plots for the neat and plasticized PLA.

neat and plasticized PLA for 1 h after being held at 185°C for 3 min to destroy any thermal history.

Polarized optical microscopy

A polarizing optical microscope (Olympus BX51) equipped with a Linkam THMSE 600 hot stage was used to investigate the spherulitic morphology and growth of the neat and plasticized PLA. The samples were first placed between glass slides and melt on a hot stage at 185°C for 3 min and then rapidly cooled at given crystallization temperature (T_c). The annealing lasted for given time periods.

Wide-angle X-ray diffraction

X-ray scattering was used to probe the crystallinity of the neat and plasticized PLA. Thin film samples were analyzed using a WAXD apparatus (Shimadzu XRD-6000) by Cu $K\alpha$ ($\lambda = 0.154$ nm) under a voltage of 35 kV and a current of 25 mA radiation. Diffraction intensities were counted at 0.02° steps, and the scanning speed was 5°/min. The spectra are recorded in an angular range $5^\circ < 2\theta < 40^\circ$ at room temperature.

RESULTS AND DISCUSSION

Equilibrium melting point

Figure 1 shows the Hoffman–Weeks plots of neat and PLA with various TPP content. The equilibrium melting point (T_m^0) was obtained from the intersection of this line with the $T_m = T_c$ equation. The T_m^0 for neat PLA was about 192.8°C, which was lower than previously reported values in the range from 198 to 212°C by Tsuji with different procedures.²⁵ The derivation might be related to the molecular weight of PLA used and experimental procedure.

The equilibrium melting point decreased largely in the early stage, but this depression was decreased with increasing TPP content. The maximum extent of this melting point depression was about 18.6°C in PLA with 30 wt % TPP content, where T_m^0 was 174.2°C. The T_m^0 of neat PLA was higher than those of plasticized PLA, indicating that the crystalline phase of neat PLA was more perfect than that of plasticized PLA.

Morphology and spherulite growth rate

Morphology

The spherulite morphology of the neat and PLA with 10 wt % TPP content crystallized at various temperatures between 100 and 142°C was examined as shown in Figures 2 and 3. The spherulitic morphologies of the neat PLA formed after isothermal crystallization at the indicated temperatures are shown in Figure 2. It was observed that the spherulites displayed the typical Maltese Cross at less than 132°C, but the distinctive Maltese Cross disappeared at 133°C. Moreover, the spherulites became irregular and distorted at higher than 134 and 140°C, respectively. For PLA with 10 wt % TPP content, as shown in Figure 3, the spherulites displayed the typical Maltese Cross at less than 119°C, but the distinctive Maltese Cross disappeared at 120°C. The spherulites became irregular and distorted at higher than 132 and 137°C, respectively. The Maltese Cross arises from the coincidence of the principle axis of the crystal with the extinction direction of the polarizer. It can easily be demonstrated that the chains are arranged circumferentially within the spherulites. The chain mobility of PLA was slow at low crystallization temperature, so the principle axis of the crystal is coincident with the extinction direction of the polarizer. However, the chain mobility of PLA speeds up and easily deviates from the principle axis of the crystal with the increase of the temperature. Moreover, the chains easily deviate from circumferential arrangement within the spherulites. So the spherulite morphology of PLA underwent a series of changes as the temperature increases. For plasticized PLA, PLA molecules moves more easily when compared with neat PLA, and the melting point of PLA declines with the addition of plasticizer, and so the variation of spherulite morphology of PLA was shifted to the lower temperature. The same thing happened to PLA with 20 and 30 wt % TPP content, but the temperatures that corresponded to the aforementioned changes were shifted to lower ones with the increase of TPP content. In the case of PLA with 20 and 30 wt % TPP content, the Maltese Cross appeared at less than 117 and 110°C and disappeared at 118 and 111°C, respectively. Meanwhile,

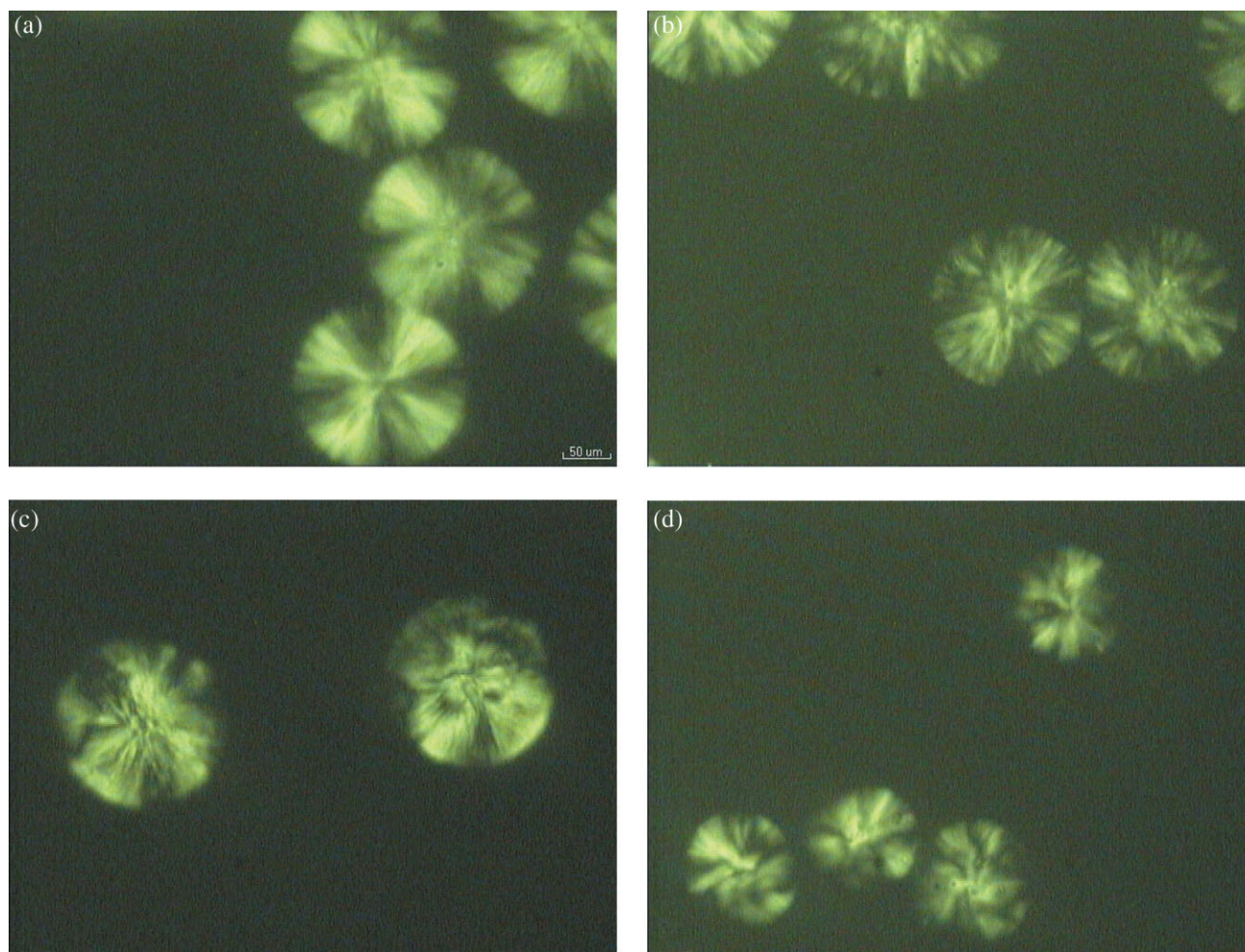


Figure 2 Polarizing optical micrographs of neat PLA crystallized isothermally: (a) 132°C, 12 min; (b) 133°C, 10 min; (c) 134°C, 10 min; and (d) 142°C, 12 min. [Color figure can be viewed in the online issue which is available at www.interscience.wiley.com.]

the spherulites became irregular at higher than 124 and 118°C and became distorted at higher than 128 and 123°C, respectively. For the sake of brevity, POM micrographs of PLA with 20 and 30 wt % TPP content are not shown in this article.

Spherulite growth rate

The spherulitic growth rates of the neat and plasticized PLA were measured by following the development of radius with time. PLA spherulites showed a linear growth until impingement takes place during the crystallization process. Figure 4 shows the temperature and component dependence of the spherulitic growth rates of the neat and plasticized PLA at different crystallization temperatures. In fact, in the case of the neat and plasticized PLA, the separate spherulite was hardly detectable because of the high nucleation density when the isothermal temperatures were low. Meanwhile, the spherulites were distorted seriously so that the size of spherulites did

not define easily when the isothermal temperatures were high. As shown in Figure 4, the spherulitic growth rates of the neat and plasticized PLA exhibited different maximum values, which corresponded to the different temperatures, and maximum values of the spherulitic growth rates were shifted to lower temperature with the increase of TPP content. From Figure 4, it can be seen that neat PLA showed a maximum value of 0.28 $\mu\text{m/s}$ for the growth rate at 132°C, and PLA with 10, 20, and 30 wt % TPP content had the maximum values of 0.51, 0.89, and 0.88 $\mu\text{m/s}$ for the growth rate at 123, 110, and 102°C, respectively. For neat PLA, initially, the spherulitic growth rate increases, then reaches a maximum value, and finally decreases at the temperature range from 123–142°C. The spherulitic growth rate of neat PLA mainly depends on the crystallization temperature (T_c). On one hand, the chain mobility of PLA increases with increasing T_c , which accelerates the spherulitic growth. On the other hand, the degree of supercooling, i.e., the difference between the

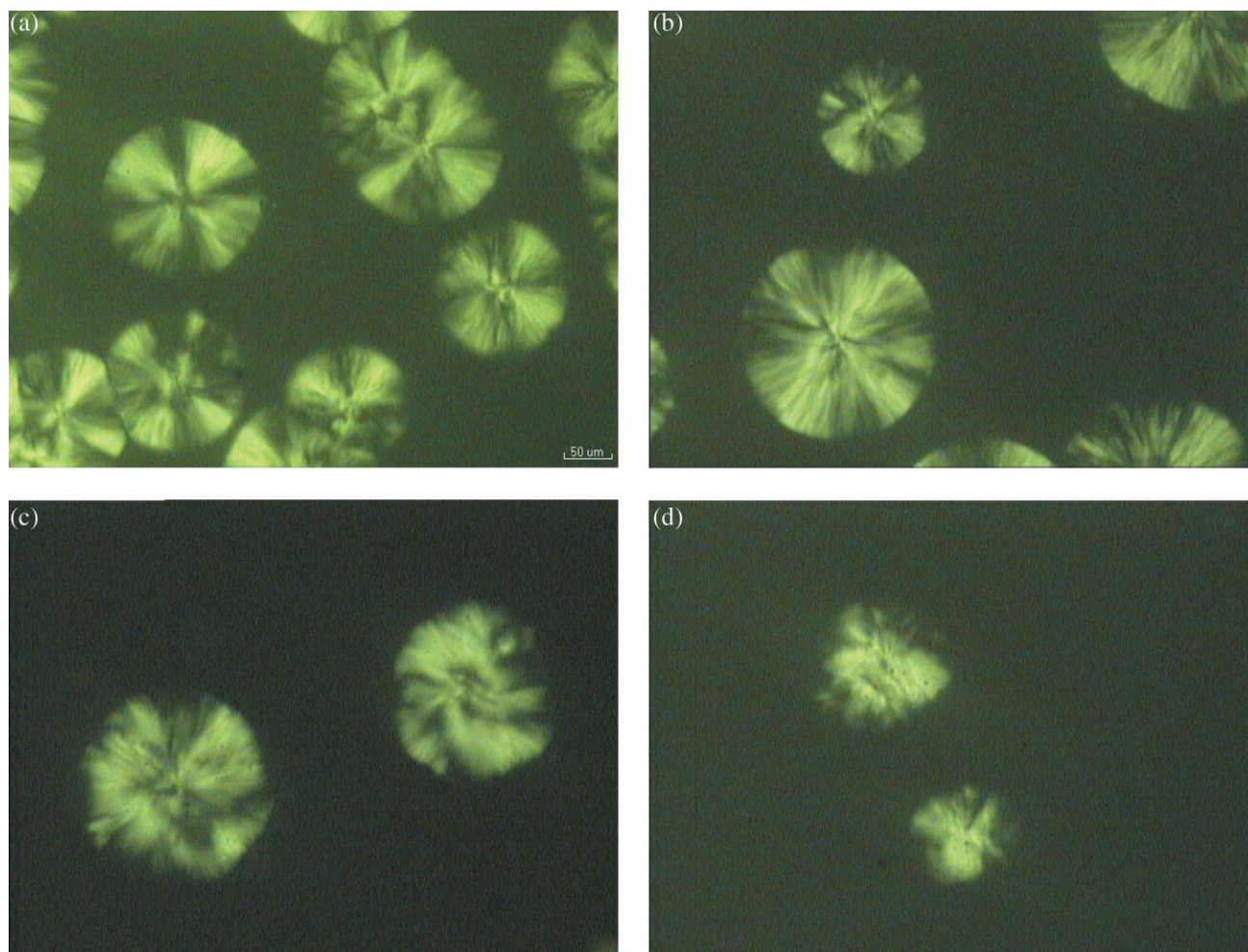


Figure 3 Polarizing optical micrographs of PLA with 10 wt % TPP crystallized isothermally: (a) 119°C, 6 min; (b) 120°C, 5 min; (c) 132°C, 10 min; and (d) 132°C, 11 min. [Color figure can be viewed in the online issue which is available at www.interscience.wiley.com.]

equilibrium melting point, T_m^0 , and the crystallization temperature, T_c , decreases with the increase of T_c , which decreases the thermodynamic driving force

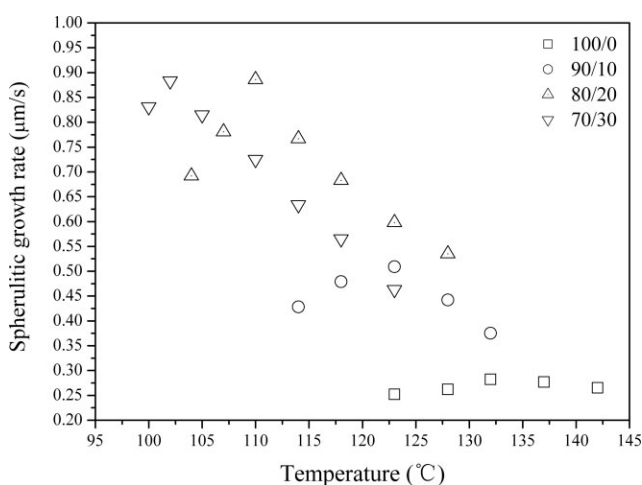


Figure 4 Temperature and component dependence of the spherulitic growth rates of the neat and plasticized PLA.

required for the growth of PLA spherulites. The variation of the spherulitic growth rates can be assigned to the combined effects of the chain mobility and the degree of supercooling. These two effects might be counteracted at lower and higher temperature, so the spherulitic growth rates were low. On the contrary, the synergic effect of the chain mobility and the degree of supercooling resulted in the maximum spherulitic growth rate of PLA at a moderate temperature. For the plasticized PLA, the variation of the spherulite growth rate against the temperature had the same tendency as the neat PLA, but the maximum values of the spherulitic growth rates were shifted to lower temperature. It might be related to the following two facts: First, the addition of low T_g -component TPP decreases the T_g of PLA, resulting in the increase of the chain mobility of PLA. Second, the addition of TPP decreases the melting point of PLA, which decreases the degree of supercooling at the same crystallization temperature. As shown in Figure 4, the spherulite growth rates of

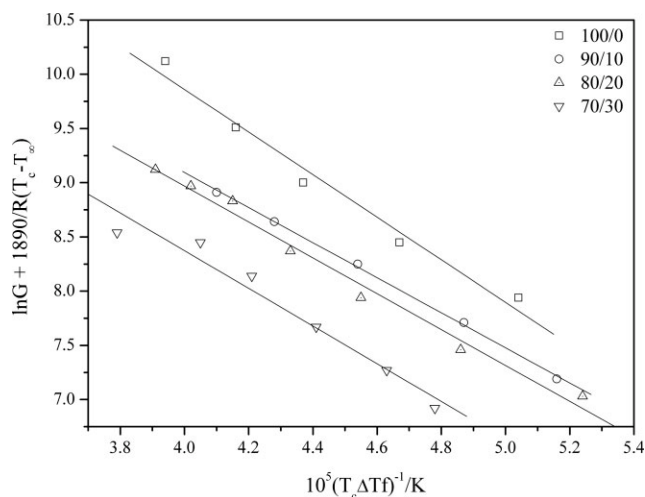


Figure 5 Plots of $\ln G + 1890/R(T_c - T_\infty)$ vs. $1/(fT_c\Delta T)$ for the neat and plasticized PLA.

plasticized PLA increased when compared with neat PLA. It can be attributed to the first effect. For PLA with various TPP contents, the maximum values of the spherulites growth rates were shifted to lower temperature with the increase of TPP content, which mainly arises from the depression of PLA's T_g , leading to the increasing of the chain mobility at lower temperature. From Figure 4, it can be found that the spherulitic growth rates of PLA with various TPP contents did not increase simply at the same temperature as TPP content increased. It might be caused by the combined effect of two factors mentioned earlier.

The famous Lauritzen–Hoffmann equation was applied to describe the spherulite growth rate in the isothermal crystallization process of the polymer for higher degrees of supercooling²⁶ as follows:

$$G = G_0 \cdot \exp\left[-\frac{U^*}{R \cdot (T_c - T_\infty)}\right] \exp\left[-\frac{K_g}{T_c \cdot \Delta T \cdot f}\right] \quad (1)$$

where U^* is the transport activation energy with a value of 1890 cal/mol,²⁷ T_∞ is a hypothetical temperature below which all viscous flow ceases ($T_\infty = T_g - 30$ K), K_g is a nucleation parameter, ΔT is the degree of supercooling, and f is a correction factor accounting for the variation in the bulk enthalpy of fusion per unit volume with temperature, $f = 2T_c/(T_m^0 + T_c)$.

Figure 5 shows the $\ln G + 1890/R(T_c - T_\infty)$ as a function of $1/(fT_c\Delta T)$, good linear relationships between $\ln G + 1890/R(T_c - T_\infty)$ and $1/(fT_c\Delta T)$ were obtained. Both K_g and $\ln G_0$ in the neat and plasticized PLA were obtained from the slope and intercept, respectively. The K_g increased with increasing TPP content, but the reverse was true for the $\ln G_0$ (Table I), implying that the incorporation of TPP increased the crystallization rate of PLA. The

TABLE I
Values of K_g , G_0 , and σ_e at Various T_c for the Neat and Plasticized PLA

PLA/TPP	$\sigma \times 10^4$ (J/m ²)	$\sigma\sigma_e \times 10^7$ (J ² /m ⁴)	$K_g \times 10^{-5}$ (K ²)	$G_0 \times 10^{-3}$ ($\mu\text{m/s}$)
100/0	3.2	1956	1.23	34.5
90/10	4.3	2633	1.62	14.5
80/20	4.4	2690	1.64	13.2
70/30	4.7	2865	1.73	7.3

fold surface-free energy (σ_e) of the growing crystal and lateral surface energy (σ) can be deduced from the following expression:

$$K_g = \frac{nb\sigma\sigma_e T_m^0}{k_B \cdot \Delta H} \quad (2)$$

where the fold surface-free energy σ_e is 6.09×10^{-2} J/m², k_B is the Boltzmann constant, b is the layer thickness (5.17×10^{-10} m), and the heat of fusion ΔH is 1.11×10^8 J/m.²⁸ The value of n may be 2 or 4, depending on the regime of crystallization spreading of new secondary nuclei at the growth front. At sufficiently high undercooling, regime III may occur, and then n is equal to 4.²⁹ Results in Table I show that the lateral surface energy of the growing crystal (σ) increased with increasing TPP content.

DSC analysis

Figure 6 shows the DSC traces of the neat and plasticized PLA at a heating rate of 10°C/min. Table II shows the glass transition temperature (T_g) of the neat and plasticized PLA as well as the cold crystallization and the melting temperatures (T_{cc} and T_m). As listed in Table II, neat PLA showed a T_g at 60.7°C, T_g s of plasticized PLA were all lower than that of neat PLA, and decreased with TPP content. The amplitude of T_g depression lied between 13.8 and 39.2°C with increasing TPP content from 10 to

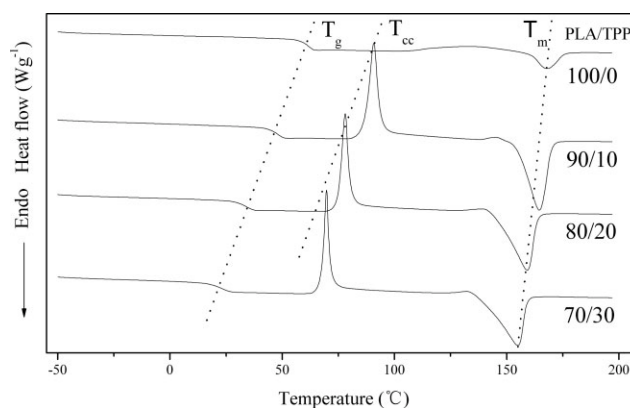


Figure 6 DSC traces of the neat and plasticized PLA.

TABLE II
Results from the Thermal Analysis of the Neat and Plasticized PLA

Weight ratios of PLA/TPP	ΔH_f (J/g)	ΔH_{cc} (J/g)	T_g , PLA (°C)	T_{cc} (°C)	T_m (°C)	x_c (%)	x_{cc} (%) ^a
100/0	12.8	—	60.7	—	167.4	13.8	—
90/10	36.6	25.6	46.9	90.8	164.7	43.8	30.6
80/20	35.3	20.2	34.2	78.2	159.1	47.4	27.2
70/30	34.2	17.0	21.5	69.2	154.9	52.5	26.1

^a The degree of cold crystallinity (x_{cc}) of plasticized PLA is calculated by eq. (3).

30 wt %. The T_g of TPP is lower than that of PLA, and the addition of TPP enhanced the segmental molecular mobility of PLA, so the T_g of PLA depressed. The melting point of PLA declined with the TPP content as listed in Table II. On one hand, the incorporation of TPP facilitates the crystallization of PLA; on the other hand, the T_m^0 of plasticized PLA also decreased. That is, crystal phase became more imperfect with the increase of TPP content. The combined effect of these two factors resulted in the depression of the melting point of PLA with the increase of TPP content.

As shown in Figure 6, for the neat and plasticized PLA, neat PLA did not display a cold crystallization peak, yet plasticized PLA did, and cold crystallization temperature decreased in parallel with the shift in T_g at the range of 69.2–90.8°C. This can be associated to two different phenomena. The first one is the increased chain mobility at low temperature associated with the larger T_g depression. This T_g reduction enables crystallization to start at an earlier temperature upon heating. A second phenomenon is the reduced crystallization induction period due to the presence of crystalline nuclei already formed during the cooling process. Even though these nuclei may represent a small crystalline fraction in absolute term, they will increase the crystallization rate upon heating since the crystalline structure is already more densely nucleated than when the polymer is being cooled from the melt. Thus, the combination of reduced T_g and higher nucleation density resulted in cold crystallization peaks, which shifted to a lower temperature as the plasticizer content was increased.

Table II shows that the neat PLA is very weakly crystallized because it presents a melting endotherm at 167.4°C with an enthalpy of 12.8 J/g in comparison with thermodynamical melting enthalpy of 93 J/g for fully crystalline PLA.²³ The degree of crystallinity was calculated based on the following equation:

$$x_c = \frac{\Delta H_f}{w_{\text{PLA}} \times \Delta H_f^0} \times 100\% \quad (3)$$

where ΔH_f is the heat of fusion, ΔH_f^0 is the heat of fusion for 100% crystalline PLA, and w_{PLA} is the

weight fraction of plasticized PLA. According to Table II, the degree of crystallinity of plasticized PLA is all higher than neat PLA. It is because the addition of TPP makes the segmental molecular mobility of PLA easier so that plasticized PLA crystallized easily. However, it is noteworthy that the degree of crystallinity obtained by eq. (3) mostly results from cold crystallization of PLA.

Crystallization kinetics

The process of the isothermal crystallization of the neat and plasticized PLA was investigated at the crystallization temperature of 114°C. The plots of the relative crystallinity X_t versus the crystallization time t are shown in Figure 7(a) for the isothermal crystallization at 114°C of the neat and plasticized PLA. It was found that except for PLA with 30 wt % TPP content, the crystallization time for the other plasticized PLA at 114°C shortened when compared with neat PLA. These results might be related to three factors: first, the addition of TPP decreased T_g of PLA, and therefore increased the chain mobility of PLA. Second, the added TPP is a diluent to PLA, resulting in the dilution of PLA chains at the spherulites growth front. Third, the decrease of the degree of supercooling depressed at the same crystallization temperature. The crystallization time shortened as TPP content was 10 and 20 wt %, indicating that the first factor was dominant. On the contrary, the addition of 30 wt % TPP lengthened the crystallization time of PLA, which might be that the crystallization rate of PLA mainly depended on the latter two factors. The well-known Avrami equation was often used to analyze the isothermal crystallization kinetics.^{30–32} It was assumed that the relative degree of crystallinity develops with crystallization time t as follows:

$$1 - X_t = \exp(-kt^n) \quad (4)$$

where X_t is the relative degree of crystallinity at time t , the exponent n is a mechanism constant with a value depending on the type of nucleation and the growth dimension, and the parameter k is a growth rate constant involving both nucleation and the

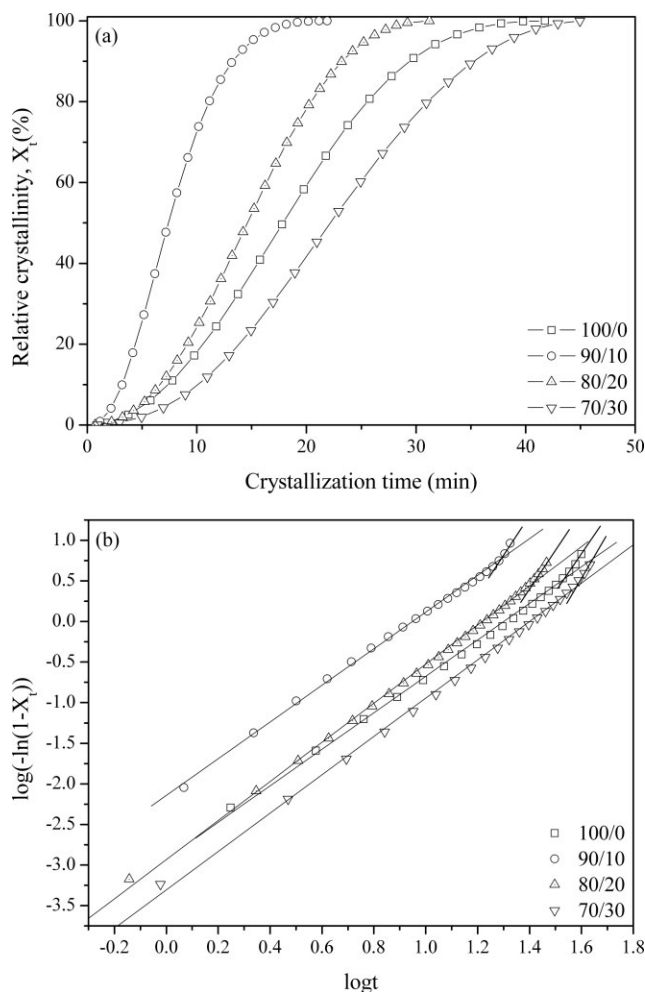


Figure 7 (a) Plots of relative crystallinity as a function of crystallization time for the neat and plasticized PLA at 114°C and (b) Avrami plots for the neat and plasticized PLA at 114°C.

growth rate parameters.³³ The plots of $\log(-\ln(1 - X_t))$ vs. $\log t$ according to eq. (4) are shown in Figure 7(b). As shown in Figure 7(b), all curves were divided into two sections: the primary crystallization stage and the secondary crystallization stage. At the primary stage, the value of n was in the range of 2.26–2.49. At the secondary stage, the Avrami exponent was in the range of 4.57–5.43. The secondary crystallization became more obvious with increasing TPP content. It was generally believed that the secondary crystallization was caused by the spherulite impingement in the later stage of crystallization process at longer crystallization time.^{34–37} As shown in Figure 7(b), the occurring time of the secondary crystallization of the neat and plasticized PLA was different. Generally, the secondary crystallization of plasticized PLA was much shorter than that of the neat PLA. This fact indicated that without the incorporation of TPP, the nucleus in neat PLA grew slowly into spherulites before they impinge against

each other. TPP caused crystallization of PLA completed earlier, because TPP accelerated the formation of PLA crystal form and then impinge against each other.

The Avrami parameters n and k were obtained from the plots of $\log(-\ln(1 - X_t))$ vs. $\log t$ as shown in Figure 7(b). The Avrami exponent n and crystallization rate constant k of the neat and plasticized PLA are shown in Table III. The average values of n were around 2.34. It is an average value of various nucleation types, and the growth dimensions occurred simultaneous in a crystallization process. For neat PLA without any heterogeneous nucleus, its nucleation type should predominantly be homogeneous nucleating and its growth dimensions should predominantly be a two-dimensional growth. For the plasticized PLA, its nucleation type should mostly be heterogeneous nucleating and its growth dimension should mostly be two-dimensional space extension. The values of n were close to 2 for the isothermal crystallization of the neat and plasticized PLA, indicating that the crystallization mechanism of PLA was almost not affected in the presence of TPP. On the other hand, the value of crystallization rate constant k of PLA with 30 wt % TPP content was decreased by one order of magnitude when compared with neat PLA, but the reverse was true for PLA with 10 wt % TPP content. The rate constant k of PLA with 20 wt % TPP content was roughly equal to that of neat PLA. These results did not seem to be in accord with those of the spherulitic growth rates at 114°C, as shown in Figure 4. It should be emphasized that overall crystallization rates were not as easy to interpret as the spherulitic radial growth because of the combination of nucleation and growth phenomena. However, the nucleation process could not be observed directly by POM.

The half-life crystallization time $t_{1/2}$, the time required to achieve 50% of the final crystallinity of the samples, is an important parameter for the discussion of crystallization kinetics. Usually, the crystallization rate is described as the reciprocal of $t_{1/2}$. The value of $t_{1/2}$ is calculated by the following equation³⁸:

$$t_{1/2} = \left(\frac{\ln 2}{k} \right)^{1/n} \quad (5)$$

TABLE III
Crystallization Kinetic Parameters of the Neat and Plasticized PLA at 114°C

PLA/TPP	n	k (min ⁻ⁿ)	$t_{1/2}$ (min)	$1/t_{1/2}$ (min ⁻¹)
100/0	2.26	2.69×10^{-4}	32.26	3.10×10^{-2}
90/10	2.24	1.51×10^{-3}	14.43	6.48×10^{-2}
80/20	2.49	2.19×10^{-4}	25.45	3.93×10^{-2}
70/30	2.37	9.77×10^{-5}	42.19	2.37×10^2

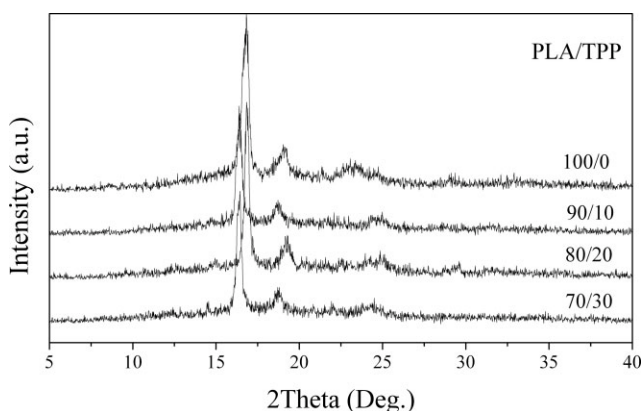


Figure 8 WAXD patterns of the neat and plasticized PLA.

where k and n are the same as in the Avrami equation. The values of $t_{1/2}$ and $1/t_{1/2}$ for the neat and plasticized PLA were calculated and listed in Table III. Comparison of neat PLA with plasticized PLA, except for PLA with 30 wt % TPP, the values of $t_{1/2}$ for plasticized PLA decreased, which indicated that the addition of excess TPP reduced the crystallization rate of PLA. Two possible reasons were proposed to explain the depression of the crystallization rate of PLA after the addition of 30 wt % TPP content. One is the presence of much TPP suppressed the nucleation of the PLA. In other words, the presence of much TPP has a negative effect on the primary nucleation of PLA. Another possible reason of the depression of the crystallization rate of PLA was probably from a physical restriction to the growth of PLA spherulites by TPP.

WAXD analysis

The diffraction traces of the neat and plasticized PLA films at room temperature are shown in Figure 8. Neat PLA presented three strong diffraction peaks at around 16.7° , 18.8° , and 23.4° , respectively.³⁹ For the plasticized PLA, they involved all the diffraction peaks corresponding to neat PLA, and the intensity of the diffraction peaks of PLA decreased with increasing TPP content. Such results indicated that plasticized PLA did not modify the crystal structure of PLA but reduced the intensity of diffraction peak.

CONCLUSIONS

The spherulitic morphology, the growth rate, and the isothermal crystallization kinetics of the neat and plasticized PLA were investigated with POM, DSC, and WAXD in detail in this work. The spherulitic morphology and growth rate were observed with hot-stage POM in a wide crystallization temperature range of $100\text{--}142^\circ\text{C}$. The spherulitic morphology and

growth rate of PLA were influenced apparently by the crystallization temperature and the TPP content. For the neat and plasticized PLA, the spherulites displayed the characteristic Maltese Cross extinction pattern in low temperature, but the Maltese Cross disappeared, became irregular and distorted with the increase of temperature. Moreover, such changes were shifted to lower temperature with the addition of TPP. The spherulitic growth rates of PLA also depended on the temperature or TPP content. The maximum values of spherulitic growth rates of plasticized PLA increased when compared with neat PLA but corresponded to lower temperature as TPP content was increased. It demonstrated that the incorporation of moderate TPP favored the spherulitic growth, which was also verified by Lauritzen–Hoffmann equation. Analysis based on the Lauritzen–Hoffmann theory showed that the values of nucleation parameter K_g increase with increasing TPP content, indicating that the incorporation of TPP accelerated the crystallization rate of PLA. Moreover, the glass transition temperature decreased and the degree of crystallinity increased sharply with the incorporation of plasticizer, showing the plasticization effect of TPP on PLA. The isothermal crystallization kinetics of the neat and plasticized PLA was studied with DSC and analyzed by the Avrami equation at 114°C . The Avrami exponent n almost remained unchangeable despite the crystallization temperature as well as the addition of TPP, indicating that PLA plasticized with TPP almost did not change the crystallization mechanism of PLA. The crystal structure of PLA was not modified by the plasticizer, and the crystal structure almost remained unchanged from the WAXD measurement.

References

- Huang, S. J. In *Encyclopedia of Polymer Science and Engineering*; Overberger, C. G., Ed.; Wiley-Interscience: New York, 1985; Vol. 2, p 220.
- Tsuji, H.; Ikada, Y. *J. Polymer* 1998, 26, 1855.
- Perego, G.; Cella, G. D.; Bastioli, C. *J. Appl. Polym. Sci.* 1996, 59, 37.
- Cai, H.; Davé, V.; Gross, R. A.; McCarthy, S. P. *J. Polym. Sci. Part B: Polym. Phys.* 1996, 34, 2701.
- Jacobsen, S.; Fritz, H. G. *Polym. Eng. Sci.* 1999, 39, 1303.
- Martin, O.; Avérous, L. *Polymer* 2001, 42, 6209.
- Hu, Y.; Hu, Y. S.; Topolkarav, V.; Hiltner, A.; Baer, E. *Polymer* 2003, 44, 5711.
- Jiang, L.; Wolcott, M. P.; Zhang, J. *Biomacromolecules* 2006, 7, 199.
- Lai, W. C.; Liao, W. B.; Lin, T. T. *Polymer* 2004, 45, 3073.
- Baiardo, M.; Frisoni, G.; Scandola, M.; Rimelen, M.; Lips, D.; Ruffieux, K.; Wintermantel, E. *J. Appl. Polym. Sci.* 2003, 90, 1731.
- Kulinski, Z.; Piorkowska, E. *Polymer* 2005, 46, 10290.
- Kulinski, Z.; Piorkowska, E.; Gadzinowska, K. *Biomacromolecules* 2006, 7, 2128.
- Piorkowska, E.; Kulinski, Z.; Galeski, A.; Masirek, R. *Polymer* 2006, 47, 7178.

14. Labrecque, L. V.; Kumar, R. A.; Davé, V.; Gross, R. A.; McCarthy, S. P. *J Appl Polym Sci* 1997, 66, 1507.
15. Ljungberg, N.; Wesslén, B. *J Appl Polym Sci* 2002, 86, 1227.
16. Ljungberg, N.; Wesslén, B. *Biomacromolecules* 2005, 6, 1789.
17. Ljungberg, N.; Andersson, T.; Wesslén, B. *J Appl Polym Sci* 2003, 88, 3239.
18. Jacobsen, S.; Fritz, H. G. *Polym Eng Sci* 1996, 36, 2799.
19. Seogjun, K.; Charles, A. W. *Polym Adv Technol* 2008, 19, 496.
20. Ji, Y. Y.; Kim, J. W.; Bae, J. Y. *J Appl Polym Sci* 2006, 102, 721.
21. Xiao, J. F.; Hu, Y.; Yang, L.; Cai, Y. B.; Song, L.; Chen, Z. Y.; Fan, W. C. *Polym Degrad Stab* 2006, 91, 2093.
22. Xiao, W. D.; He, P. X.; Hu, G. P.; He, B. Q. *J Fire Sci* 2001, 9, 369.
23. Fisher, E. W.; Sterzel, H. J.; Wegner, G.; Kollid, Z. Z. *Polymer* 1973, 25, 980.
24. Hoffman, J. D.; Weeks, J. J. *J Res Natl Bur Stand Sect A* 1962, 66, 13.
25. Tsuji, H.; Miyauchi, S. *Polym Degrad Stab* 2001, 71, 415.
26. Lauritzen, J. I.; Hoffman, J. D. *J Appl Phys* 1973, 44, 4340.
27. He, Y.; Fan, Z. Y.; Wei, J.; Li, S. M. *Polym Eng Sci* 2006, 46, 1583.
28. Vasanthakumari, R.; Pennings, A. J. *Polymer* 1983, 24, 175.
29. Hoffman, J. D. *Polymer* 1983, 24, 3.
30. Avrami, M. *J Chem Phys* 1941, 9, 177.
31. Tobin, M. C. *J Polym Sci Polym Phys Ed* 1974, 12, 399.
32. Tobin, M. C. *J Polym Sci Polym Phys Ed* 1976, 14, 2253.
33. Avrami, M. *J Chem Phys* 1939, 7, 1193.
34. Wunderlich, B. *Macromolecular Physics*; Academic Press: New York, 1977; Vol. 2.
35. Liu, J. P.; Mo, Z. S. *Chin Polym Bull* 1991, 4, 199.
36. Liu, T.; Mo, Z.; Wang, S.; Zhang, H. *Polym Eng Sci* 1997, 3, 568.
37. Dell'Erba, R.; Groeninckx, G.; Maglio, M.; Malinconico, M.; Migliozi, A. *Polymer* 2001, 42, 7831.
38. Di Lorenzo, M. L.; Silvestre, C. *Prog Polym Sci* 1999, 24, 950.
39. Ueda, A. S.; Chatani, Y.; Tadokoro, H. *Polym J* 1971, 2, 387.